

## Numerical Modeling of Advection and Diffusion of Urban Area Source Pollutants

BRUCE A. EGAN AND JAMES R. MAHONEY

*Dept. of Environmental Health Sciences, Harvard School of Public Health, Boston, Mass. 02115*

(Manuscript received 22 July 1971, in revised form 8 November 1971)

### ABSTRACT

A numerical, grid-element model has been developed for the study of air pollution transport from urban area-type sources. This advection-diffusion model is especially useful for the estimation of air pollution concentrations under conditions of spatial and time varying emissions, velocities and diffusion rates. The "pseudo-diffusive" errors associated with conventional finite-difference approximations to advective transport are eliminated by a material-conserving computation procedure involving the zeroth, first and second moments of the concentration distribution within each grid element. Extensions of the procedure are suggested for retention of sub-grid-scale resolution of concentration values necessary in the study of transport of chemically reactive materials, or for the incorporation of emissions from point and line sources. A novel procedure is presented for the numerical simulation of horizontal diffusion from area sources which can be used to model empirically observed dispersive growth rates.

### 1. Introduction

Urban pollutants are emitted by a very large number of sources of highly variable strength. To estimate resulting air pollution concentrations with meteorological dispersion models it is appropriate to separate the largest sources which may have well-documented emission rates, stack heights, etc., from the multitude of smaller sources whose individual emission characteristics are not so well known. For efficiency, it is desirable to treat emissions from these latter sources mathematically as area or shallow-volume type sources. These sources have emission rates averaged over dimensions determined by consideration of the spatial resolution of the available source inventory, and the desired resolution of the concentration distribution to be calculated. For a large urban region, the scale of a source element might be of the order of 500–2000 m in horizontal dimension and, if a volume type, of order 10–100 m high.

This paper describes a numerical advection-diffusion model which specifically treats the transport of emissions from large shallow-volume sources, and represents further developments of transport models previously reported by Mahoney and Egan (1971) and Egan and Mahoney (1971). These models are particularly useful for the investigation of short-term changes in emission strengths and meteorological parameters and thus constitute an appropriate tool to investigate transport of pollutants by local circulations, advection of air masses of varying stability characteristics, fumigation, and other time- and space-dependent phenomena. The models can be easily adapted to a number of applications, and can serve as building blocks for detailed

simulations in three dimensions, for studies of the transport of reacting materials, and for link-up type models to incorporate statistical dispersion estimates of emissions from point and line sources.

This paper: 1) deals in detail with the problem of simulating the advective and diffusive processes without incurring large artificially introduced truncation errors; 2) extends the numerical procedures adopted so that information of sub-grid-scale concentration detail (e.g., emissions from line or point sources) can be retained; 3) extends the advection procedure for application to a two-dimensional horizontal wind field; and 4) presents a unique form for simulating horizontal diffusion from area sources. The numerical schemes adopted fundamentally conserve pollutant material and descriptive statistics of the material distribution. Consequently, in contrast to many other types of models for area sources, calculation results can be easily interpreted in terms of the physical processes involved in the transport of the emissions.

### 2. Related work

A variety of meteorological and statistical models are available to estimate air pollution concentrations within urban areas. Recent summaries of computational techniques and results of model calculations have been prepared by Moses (1970), Mahoney (1970) and Neiburger and Chin (1970). Detailed descriptions and discussions of several models in current use appear in Stern (1970). Most of these models are based on multiple applications and extensions of the empirically based Gaussian plume-type of calculation developed for point-

source emissions by Pasquill (1961) and modified by Gifford (1961) and Turner (1969).

The integration of the Gaussian kernel over an area source has not been done analytically. Thus, in order to use the Gaussian form and its supporting data, the area-type source is commonly approximated by a point source of the same strength, perhaps located some distance upwind, or by one or more finite length line sources. Calder (1970) has reviewed several approaches and pointed to the need for more accurate approximations to area-source dispersion. This need is most apparent when small-scale variations of concentrations within an urban area are to be estimated. The simple approximations to source geometry only yield accurate estimates many grid widths downwind of the source.

Among the more refined approaches to area-source emissions is that of Fortak (1970) who approximated an area source by a fine mesh of point sources and created an inventory of concentration fields for different combinations of meteorological parameters for use in the model calculations. Shieh *et al.* (1970) developed algorithms from numerical integrations of the Gaussian kernel to describe quasi-steady dispersion relationships for area sources.

Advection and diffusion of true area-source emissions can be handled more directly when recourse is made to partial differential equations describing the transport, using eddy diffusivities as gradient transfer coefficients. These equations are most applicable to the description at atmospheric transport when horizontal dispersion rates are not of major importance. This is especially the case for emissions from cross-wind line sources, but adaptation to the description of area-source emissions can be made by formally employing the "narrow plume hypothesis" (Calder, 1969a) to neglect horizontal diffusion. Gifford and Hanna (1971) have successfully employed this hypothesis and parameterized wind and diffusivity distributions in the vertical to develop a simple area-source model for the estimation of time-averaged concentration patterns. Although analytic solutions to the advection-diffusion equations exist for some simple geometries and distributions of wind and vertical eddy diffusivity (see especially Pasquill, 1961), it is generally necessary to use numerical techniques to estimate air pollution concentrations. Procedures to obtain steady-state numerical solutions for line-source emissions for a variety of boundary conditions have been developed and discussed by Calder (1969b) and Wallington (1968). The variability of the meteorological characteristics associated with urban areas has provided special motivation for the use of numerical models capable of incorporating spatial and temporal variations. Application of numerical modeling techniques to urban areas has been made by Sklarew (1970) utilizing a mixed Eulerian and Lagrangian description to advect and diffuse particles representing pollutant emissions throughout a grid system, and by Randerson (1971) who applied more conventional finite-

difference techniques to describe the steady-state transport of SO<sub>2</sub> with topographically induced vertical velocities.

### 3. Application of the transport equation to urban area source emissions

Advection and diffusion of a conservative pollutant in an incompressible fluid is described by the tracer equation

$$\frac{\partial C}{\partial t} = -\mathbf{U} \cdot \nabla C + \nabla \cdot K \nabla C. \quad (1)$$

In a numerical simulation based on (1), emissions from finite geographical areas can be modeled as shallow volume sources which are more appropriate than surface-based area sources for treating near-surface emissions in urban areas. The shallow volume becomes a ground-level grid element in the numerical scheme.

In marked contrast to the application of "K theory" to dispersion from point sources, the use of the advection-diffusion equation to describe transport from volume-type sources seems especially appropriate. A plume from a point source can undergo a change of cross-wind scale of the order of 1000:1 traveling across an entire urban region. Over the course of its transport it is dispersed by a wide range of eddy sizes; the smallest eddies are important to the initial mixing; later, as the plume grows in size, the larger eddies are more important. Turbulent mixing by a wide spectrum of eddy sizes and eddy velocities cannot be described by a single value of an eddy diffusion coefficient. Dispersion by a constant value of  $K$  requires that plumes grow as the half-power of downwind distance. In reality, plumes grow more nearly linearly with distance except under very stable conditions. Emissions from a shallow-volume source undergo a much smaller change of scale as they are transported downwind the same distance. Because the scale of the source is initially large, the small-scale eddies will not be important to the dispersion. When the range of eddy sizes responsible for mixing is reduced and when the relative plume growth is small, a single value of  $K$  can provide a much better description of the dispersive growth rate.

Panofsky (1969) and Pasquill (1970) have pointed out that the gradient-transfer approach to atmospheric diffusion is most likely to be successful when applied to the vertical dispersion of emissions from ground level. When only vertical dispersion is considered, the scale of the largest eddies important to the mixing is limited by the proximity to the ground. Specification of a  $K$  increasing with height can model this effect.

### 4. Description of the numerical model in two dimensions

The main features of the numerical model can be described by reduction of the tracer equation to two-

dimensional form. For simplicity, vertical velocities are neglected. If comparable resolution of concentration values is required for the horizontal and vertical, diffusion in the direction of horizontal flow can be neglected.

The two-dimensional equation describing the changes of concentrations resulting from horizontal advection and vertical mixing is

$$\frac{\partial C}{\partial t} = -U \frac{\partial C}{\partial x} + K \frac{\partial^2 C}{\partial z^2} + Q, \quad (2)$$

where  $Q$  denotes addition of contaminant material per unit volume and time.

#### a. Specification of initial values and boundary conditions

Initial values of the concentration field are often set equal to zero, and steady- or quasi-steady-state solutions are generated from rest. For application to short-term forecasting, current air quality measurements can be used as initial values. Concentrations at the upwind edge of the computational grid must be externally specified at all times. Boundary conditions must also be applied at the bottom and top of the grid because of the vertical diffusion term. At the bottom, it is convenient to specify a reflection coefficient to simulate the effect of a partially absorbant barrier. The top of the grid system can often be set high enough so that concentrations there will be small fractions of lower level concentrations. In this way the calculation solution will be insensitive to the boundary condition (reflection coefficient) chosen for the top. Inversions can be modeled by setting the vertical diffusion coefficient to a small value at the appropriate altitude.

#### b. Numerical simulation of transport using grid elements

To simulate transport the model region is divided into a number of grid elements, and the spatial derivatives in (2) are approximated by finite differences corresponding to the dimensions of the grid elements. Scaling arguments suggest that the elements be elongated in the horizontal and shallow in the vertical. Time derivatives are approximated by forward-difference increments.

Emissions from area-type sources are introduced to the lowest level grid elements of the model each time step. The scale of the source inventory determines the minimum grid sizes useful for resolution of concentrations values. Large concentration differences can occur between adjacent grids; thus, the difference scheme adopted must be accurate for high wavenumber variations of concentrations. Horizontal advection and vertical diffusion in (2) are mathematically separable, and for convenience in computation, the finite-difference simulation is performed in two separate, sequential steps.

#### c. Treatment of horizontal advection

Many finite-difference schemes can be used to evaluate Eq. (2); all are inaccurate to some degree. Finite-difference approximations to the advective part of (2), in particular, introduce errors of both phase and amplitude. Investigations by Molenkamp (1968) and Crowley (1968) comparing the relative accuracy of alternative computation schemes for the advection equation show that truncation errors can be suppressed by multiple-step or high-order schemes requiring the use of several upwind and downwind concentration values at each calculation. These schemes are computationally expensive and, even among the most accurate, the errors generally become large when the wavelength of spatial variations approaches the grid element dimension. The amplitude and phase of the truncation errors also vary with the parameter,  $\sigma = U\Delta t/\Delta x$ , which is the ratio of the advection distance per time step to the grid element dimension.

With the large grid spacing required for computational economy (and satisfactory for treatment of urban-scale pollution phenomena), upwind-downwind mixing of material by numerical "pseudo-diffusion" arising from simple difference schemes can be orders of magnitude larger than mixing by real atmospheric diffusion. The existence of large errors at high wavenumbers, and the variability of errors as a function of local velocity are undesirable characteristics for a "building block" model of urban area source-emitted air pollution.

Because the concentration values are not coupled to the driving fluid dynamics, a numerical scheme which maintains sharp intercellular concentration gradients is acceptable. With this in mind, we have adopted the unconventional scheme described below to suppress pseudo-diffusive effects in simulating the advective term in (2).

#### d. One-dimensional horizontal advection using moments of the concentration distribution

The pseudo-diffusion associated with numerical advection can be reduced substantially (to zero in some cases) by utilization of one or more moments of the concentration distribution within a grid element in the computation scheme. Motivation for the procedure emerges from a consideration of the mechanism generating the numerical diffusion.

The forward-time, backward-space, finite-difference approximation to the advective part of (2) for  $U > 0$  is

$$C_{m,n}^{T+1} = (1-\sigma)C_{m,n}^T + \sigma C_{m-1,n}^T, \quad (3)$$

where  $T$  denotes the  $T$ th time step such that  $t = T\Delta t$  and  $m$  and  $n$  denote the  $m$ th horizontal and the  $n$ th vertical grid elements such that  $x = m\Delta x$  and  $z = n\Delta z$ . Computational stability requires that  $\sigma \leq 1$ . Fig. 1a compares the transport of material by the "real"

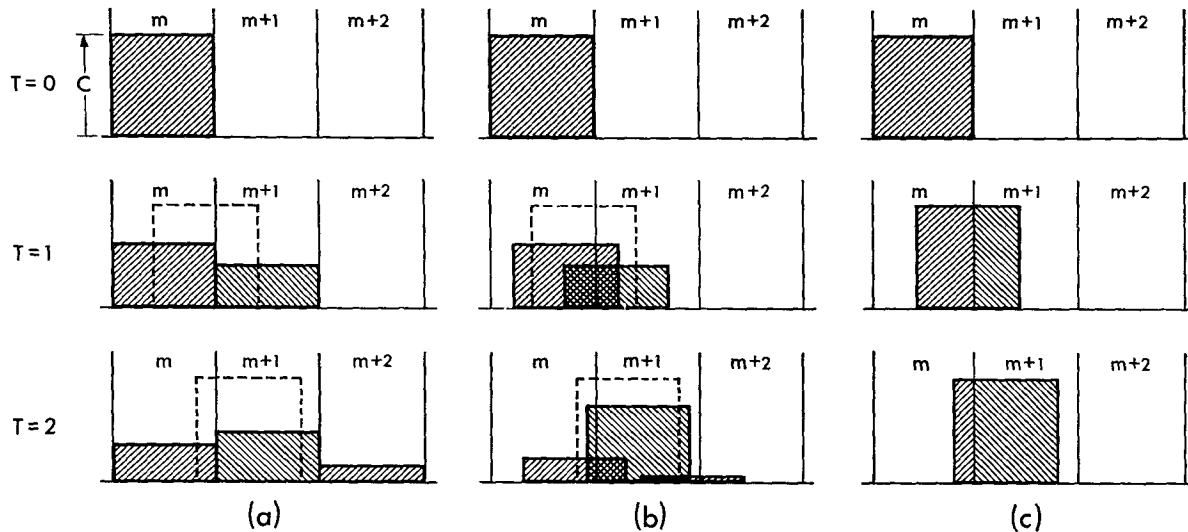


FIG. 1. An initially rectangular concentration distribution advected to the right in three sequential time steps with  $\sigma=0.4$ . Dashed distribution corresponds to transport by continuum advection. (a) Simple finite-difference [Eq. (3)]. (b) Difference scheme using reconstruction with first moment of concentration distribution. (c) Difference scheme using reconstruction with first and second moments.

advection process with that by Eq. (3) for three sequential time steps. Advection by (3) occurs by propagation of material to the center of the downwind grid cell and subsequent mixing throughout the cell each time step. Some material always remains in the original cell. In the real advective process, material is transported only part way into the downwind cell and does not overtake any of the material originally in the downwind cell. After many time steps, the numerical scheme of (3) can be likened to advection with velocity  $U$  and upwind-downwind diffusion with a "pseudo-diffusion" coefficient of magnitude  $U\Delta x(1-\sigma)/2$ .

The interpretation of the mechanism of pseudo-diffusion in the simple finite-difference scheme suggests that a reduction in the diffusive effect can be achieved if the center of mass or the first moment  $F$  of the material within a cell is calculated after each time step and is used to adjust the amount of material advected downwind the next time step. Advection using reconstruction of the first moment is illustrated in Fig. 1b. The mathematics involved, described previously (Egan and Mahoney, 1971), is omitted here as it is a degenerate case of the procedure to be described below. A substantial further reduction in the pseudo-diffusion effect may be achieved by calculating the second moment of the concentration distribution in each cell after each time step. This moment sizes the distributions horizontally within each grid cell and thus allows suppression of the diffusive effect of overlapping distributions. Specifically, the procedure calculates the first and second moments of the concentration distribution after material has been advected into and out of a grid element. These moments are then used to construct a simple rectangular distribution in the element having the same amount of material and identical first and second moments.

The second moment evaluated about the center of mass is the radius of gyration, or equivalently, the square root of the variance,  $V^2$ , of the material distribution. For a rectangular distribution of length  $L$ , it has the value  $L/\sqrt{12}$ . Thus, a convenient scale of the horizontal extent of an arbitrary distribution within a grid element is  $R=\sqrt{12}V/\Delta x$ . Then, for a rectangular distribution,  $R=L/\Delta x$ .

Suppressing vertical subscripts, we let  $\xi_m$  denote the relative displacement of material within the  $m$ th cell from the center of the cell, such that  $\xi_m$  ranges from  $-0.5$  to  $+0.5$  at the left- and right-hand extreme boundaries of a cell, and we normalize all length dimensions by the grid element width  $\Delta x$ . The zeroth, first and centered second moments of the grid cell concentrations distribution corresponding to the mean concentration, the center of mass, and the scaled distribution variance are given by

$$C_m = \int_{-0.5}^{0.5} C(\xi_m) d\xi, \quad (4)$$

$$F_m = \int_{-0.5}^{0.5} C(\xi_m) \xi_m d\xi / C_m, \quad (5)$$

$$R_m^2 = \int_{-0.5}^{0.5} C(\xi_m) (\xi_m - F_m)^2 d\xi / C_m. \quad (6)$$

For simple rectangular concentration distributions, these integrals are readily evaluated by summation for each grid element in terms of the material distributions of the portions remaining and newly-advected in after each successive time step. Fig. 2 illustrates the advection of a step-shape distribution the fractional distance

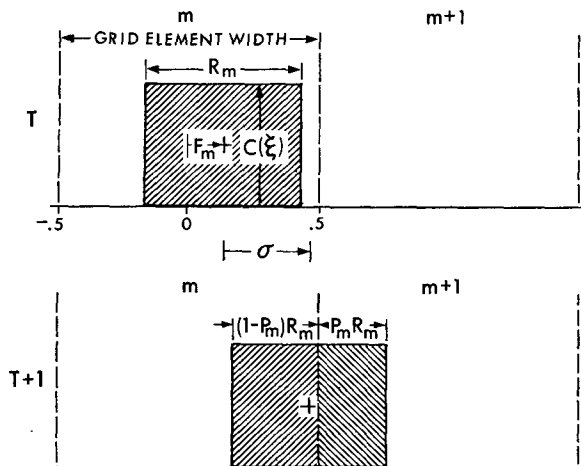


FIG. 2. Scale parameters involved in advection of a rectangular concentration distribution downwind in one time step.

$\sigma$  in one time step. It may be seen that the nature of the downwind transfer depends upon the value of the portioning parameter  $P_m = (F_m + \sigma + R_m/2 - 0.5)/R_m$ . For  $P_m \leq 0$  none of the material is advected into the  $m+1$  cell. If  $P_m \geq 1.0$  all the material is advected into the downwind cell. For  $1 > P_m > 0$ , an amount of material  $P_m C_m$  is advected to the downwind cell and  $(1 - P_m)C_m$  remains in the  $m$ th cell. For this latter, most general case, the material advected downwind will have a center of mass at  $-0.5 + (P_m R_m/2)$  relative to the center of the  $m+1$  cell and will have a horizontal extent equal to  $P_m R_m$ . Similarly, the amount remaining in the  $m$ th cell will have a center of mass at  $(1 - R_m + P_m R_m)/2$  and a horizontal extent  $(1 - P_m)R_m$ .

Considering now the general case for the  $m$ th cell with inflow from the  $m-1$  cell, outflow to the  $m+1$  cell, and continuous source addition during the time step, the forward-time computation procedure at grid element  $m$  can be represented as

$$C_m^{T+1} = C_r + C_a + Q\Delta t, \quad (7)$$

$$C_m^{T+1} F_m^{T+1} = C_r F_r + C_a F_a + Q\Delta t(\sigma/2), \quad (8)$$

$$C_m^{T+1} (R^2)_m^{T+1} = C_r [R_r^2 + 12(F_m^{T+1} - F_r)^2] \\ + C_a [R_a^2 + 12(F_m^{T+1} - F_a)^2] \\ + Q\Delta t [1 + 12(F_m^{T+1} - \sigma/2)^2], \quad (9)$$

where subscripts  $r$  and  $a$  indicate quantities remaining and newly-advected in, respectively. These quantities can be evaluated from the portioning parameter,  $P_m$ ,

using the following rules:

$$\text{if } P_m < 0: \quad C_r = C_m^T, \quad F_r = F_m^T + \sigma, \quad R_r = R_m^T$$

$$\text{if } P_{m-1} < 0: \quad C_a = 0, \quad F_a = 0, \quad R_a = 0$$

$$\text{if } P_m > 1: \quad C_r = 0, \quad F_r = 0, \quad R_r = 0$$

$$\text{if } P_{m-1} > 1: \quad C_a = C_{m-1}^T, \quad F_a = F_{m-1}^T + \sigma - 1, \quad R_a = R_{m-1}^T$$

$$\text{if } 0 < P_m < 1: \quad C_r = (1 - P_m)C_m^T,$$

$$F_r = (1 - R_m^T + P_m R_m^T)/2, \quad R_r = (1 - P_m)R_m^T$$

$$\text{if } 0 < P_{m-1} < 1: \quad C_a = P_{m-1}C_{m-1}^T,$$

$$F_a = (P_{m-1}R_{m-1}^T - 1)/2, \quad R_a = P_{m-1}R_{m-1}^T$$

The step-shaped concentration distribution will be advected downwind without change of shape as illustrated in Fig. 1c. Thus, the procedure completely eliminates pseudo-diffusive effects in this case. Small diffusive errors will remain when more complicated distributions are advected. Complex shapes will, after many time steps, degenerate to a simple rectangular shape with the same second moment. In all cases, reconstruction with the first and second moments conserves the variance of the entire concentration distribution as it is advected.

The procedure reduces to the first-moment system (illustrated in Fig. 1b) if all  $R$ 's are set to unity and to the zeroth-moment system [Eq. (3) and illustrated in Fig. 1a], if, in addition, all  $F$ 's are set to zero.

#### e. Treatment of vertical diffusion

The vertical diffusion component of Eq. (2) is simulated by a conventional forward-time, centered-difference technique modified so that variable grid spacing can be specified in the vertical. In regions where parameters or concentrations change rapidly with height, resolution and accuracy can be improved with smaller vertical grid spacing. In other regions (typically at high altitude) where gradients are smaller, large grid spacings can be used.

The calculation may be represented by

$$C_n^{T+1} = (1 - \alpha_{n+1} - \alpha_{n-1})C_n^T + \alpha_{n+1}C_{n+1}^T + \alpha_{n-1}C_{n-1}^T, \quad (10)$$

where the horizontal subscript  $m$  is now suppressed, and

$$\alpha_{n+1} = \frac{(K_n + K_{n+1})\Delta t}{\Delta z_n(\Delta z_n + \Delta z_{n+1})}, \\ \alpha_{n-1} = \frac{(K_n + K_{n-1})\Delta t}{\Delta z_n(\Delta z_n + \Delta z_{n-1})}. \quad (11a, b)$$

The diffusion coefficients  $K_n$  are evaluated at the center of the grid elements, and  $\Delta z_n$  denotes the depth of the  $n$ th grid element. Computational stability is

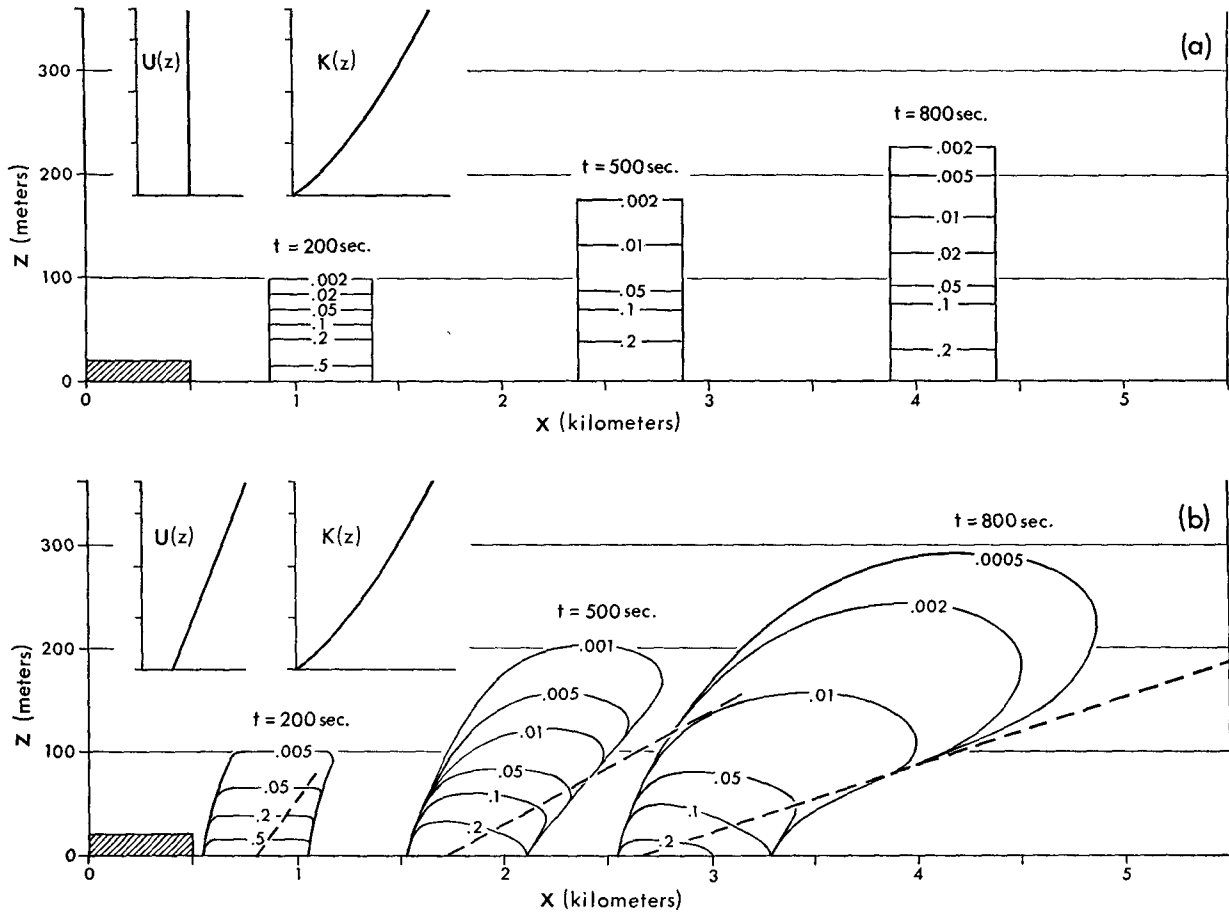


FIG. 3. Concentration isopleths for dispersion of a volume-source puff of unit initial concentration with time. Shaded areas in lower left corners are the volume-source elements. Wind and diffusivity profiles are shown in reduced scale as inserts. (a) Uniform velocity. (b) Velocity increasing linearly with height; dashed line for each travel time shows product of time and local velocity.

maintained if the  $\alpha$ 's are less than 0.5. When  $n$  corresponds to the top and bottom boundary cells of the grid system, the  $\alpha$ 's take on values

$$\alpha_{n+1} = (1 - r_{\text{top}})\alpha_{n-1}, \quad \alpha_{n-1} = (1 - r_{\text{bottom}})\alpha_{n+1},$$

respectively, where  $r$  is a "reflection coefficient" between 0 and 1, allowing a simple simulation of absorption or loss of material from the grid system.

When high resolution of concentration values in the horizontal is desirable, the first and second moments of the horizontal distribution can be maintained in the diffusive transfer by two additional equations:

$$F_n^{T+1} = [C_n^T F_n^T (1 - \alpha_{n+1} - \alpha_{n-1}) + \alpha_{n+1} C_{n+1}^T F_{n+1}^T + \alpha_{n-1} C_{n-1}^T F_{n-1}^T] / C_n^{T+1}, \quad (12)$$

$$(R^2)_n^{T+1} = \{C_n^T [(R^2)_n^T + 12(F_n^T - F_n^{T+1})^2] (1 - \alpha_{n+1} - \alpha_{n-1}) + \alpha_{n+1} C_{n+1}^T [(R^2)_{n+1}^T + 12(F_{n+1}^T - F_{n+1}^{T+1})^2] + \alpha_{n-1} C_{n-1}^T [(R^2)_{n-1}^T + 12(F_{n-1}^T - F_{n-1}^{T+1})^2]\} / C_n^{T+1}. \quad (13)$$

#### f. Application to the dispersion of a volume-source puff

Test case examples of two-dimensional calculations using the above procedures are illustrated in Fig. 3. Isopleths of concentration of material originating as a 50-sec duration puff from a ground-level shallow-volume source are shown for increasing travel times. In Fig. 3a the horizontal velocity is constant with height at a value of  $5 \text{ m sec}^{-1}$ , and the vertical diffusion coefficient is arbitrarily given as a function of height by  $K(z) = 0.16z^{0.75} [\text{m}^2 \text{ sec}^{-1}]$ , where  $z$  is in meters. The material diffuses vertically and is simply transported downwind a distance equal to the product of velocity times the travel time. With the elimination of the numerically produced pseudo-diffusion there is no spreading in the upwind-downwind distribution. In the absence of a velocity gradient, the distribution of material in the vertical can be compared with the corresponding one-dimensional analytic solution to an instantaneous finite-depth source of equivalent strength. This is shown in Fig. 4.

Fig. 3b has the same vertical diffusion field but the horizontal velocity is given by  $U(z) = 3 + 0.02z [\text{m sec}^{-1}]$ .

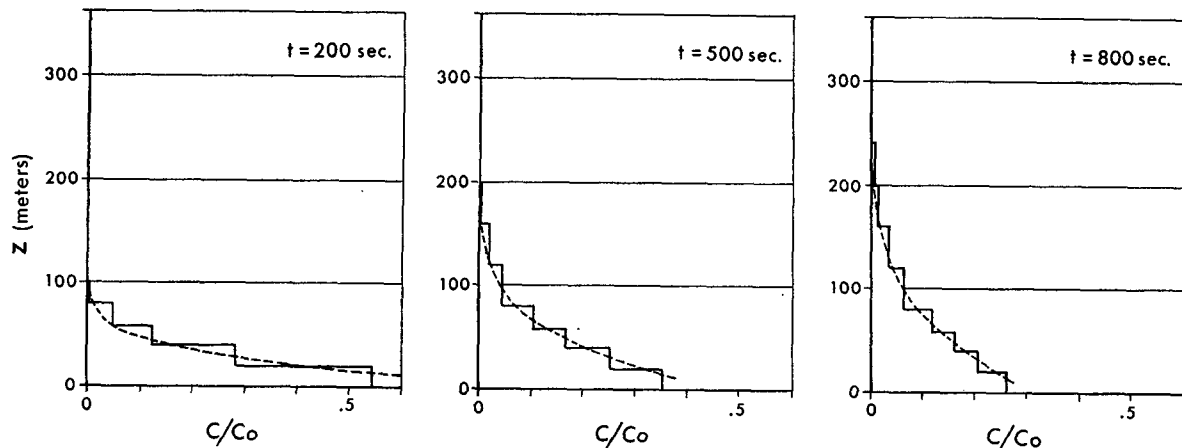


FIG. 4. Comparison of computed vertical concentration distributions with the analytic solutions (dashed lines) for dispersion of an instantaneous volume source of equivalent strength.

It was not possible to obtain an analytic result for comparison in the case of a vertically varying wind field. However, it is interesting to note two effects of the velocity gradient on the material distributions. First, there is now some upwind-downwind spreading of material associated with displacement by shearing and subsequent redistribution by vertical diffusion. Secondly, the centroids of the distributions in the upwind-downwind direction no longer coincide with the product of the velocity times travel time (shown as dashed lines), a result of the finite rates of upward diffusion of material. It may be shown, however, that the vertical distribution of material integrated along the wind direction is the same for Figs. 3a and 3b, a result of the separable nature of solutions to (2).

*g. Use of higher moments for preservation of sub-grid-scale details*

The procedure of characterizing the distribution of concentrations within a grid element by its moments or other available scale parameters will generally lead to still further reduction of numerical diffusion as more scaling parameters are introduced, allowing reconstruction of distributions with additional degrees of freedom. The degree of refinement of the distribution reconstruction required will vary among applications. Carrying the first and second moments only in the procedure generally insures that truncation errors associated with the advection term are at least as small as errors associated with the finite-difference approximations to the diffusion terms.

In application to urban air pollution transport there are situations where preservation of sub-grid-scale detail by more moments in the advection process, as illustrated in Fig. 5, is desirable. These situations include:

1) Resolution of concentration distribution details when large background levels exist.

2) Inclusion of line-type source emissions. Contributions from cross-wind line sources (of finite width less than the area source grid width) can be added as rectangular bumps of additional material. Line sources aligned with the wind can be treated similarly in three dimensions.

3) "Link-up" with plumes from large point sources. The initial dispersion of emissions from large point sources is best treated in a separate, parallel calculation (e.g., Gaussian plume format). To make best use of the specified variable wind and diffusivity fields, we would like to incorporate the contributions from the point sources into the numerical advection scheme. This can be accomplished in a three-dimensional model after the plume has grown sufficiently large to be approximated by a few shallow regions of uniform concentration. Since the vertical grid element spacing is generally much smaller than the horizontal, the addition of a plume concentration to the existing concentrations within each grid element could be represented by a rectangular ridge aligned with the flow, with dimensions determined by the statistical characteristics of the plume.

4) Chemical interactions where reaction rates depend upon concentrations. When transport of chemically reacting species is modeled, it may be necessary to retain details of the local concentration distribution to estimate reaction rates.

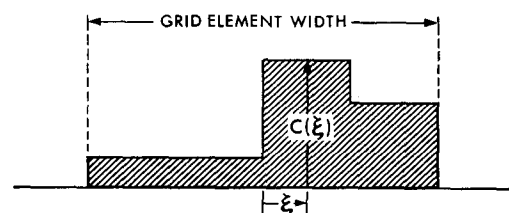


FIG. 5. An example of a concentration distribution requiring additional moments to preserve sub-grid-scale detail during numerical advection.

Preservation of sub-grid-scale concentration detail by the method of retaining higher moments represents an alternative to simply reducing the grid sizes in the model. Reduction of grid size will increase the total number of grid elements needed to represent the region, and, for forward-time step explicit procedures, will generally necessitate a reduction of the incremental time steps. The increased computation cost associated with retention of higher moments of the concentration distributions may compare favorably with the increased costs associated with reduction of grid size.

### 5. Extension to three-dimensional models of advection and diffusion of area-source emissions

The procedures outlined for the two-dimensional model can be easily extended to include horizontal diffusion and advection by a three-dimensional wind field. It is important to note that the increased accuracy of description expected from complete simulation in three dimensions may not be sufficient to justify the necessary additional complexity in the computations. For many applications where strong convergence or divergence of the wind fields is not present, the neglect of the vertical component of velocity in the transport simulation will be justifiable. Near-ground-level emissions from area sources will tend to remain at ground level, and the major effects of orography could probably best be simulated by modification of the horizontal wind directions.

Because the plume from a shallow volume-source element has large initial horizontal dimensions, it will grow relatively slowly during transport over an urban region. The reduced relative dilution for area sources implies that it is more important to specify the trajectories of the emissions, rather than the horizontal dispersion rate. In the dispersion model for Connecticut, Hilst (1970) has demonstrated the relative insensitivity of concentration values to variations in the horizontal dispersion coefficient, and the sensitivity to variations in the horizontal velocity field. This result is expected to be found in urban scale models also.

If source strength varies slowly within the urban area, the net effect of horizontal mixing upon the concentration distribution will be further reduced. In terms of overall accuracy, proper treatments of horizontal advection and vertical diffusion processes are of primary importance, and the treatment of horizontal diffusion is of secondary importance. Two-dimensional horizontal advection and diffusion are discussed separately in the next two sections.

#### a. Extension of moment method to horizontal advection in two dimensions

The second-moment method can be applied to suppress pseudo-diffusive errors in modeling two-dimensional advection. Fig. 6 illustrates in top view the

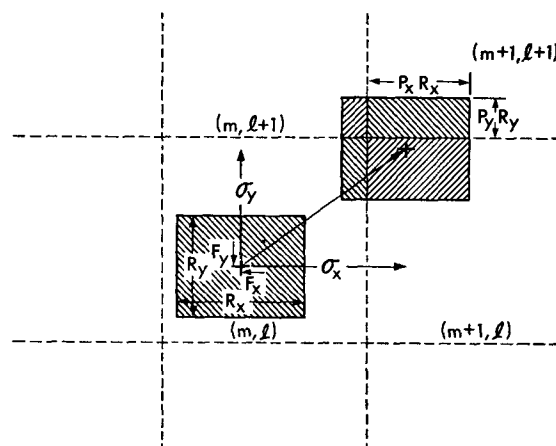


FIG. 6. Scale parameters involved in the advection of rectangular block of material of uniform concentration from a position within the  $m, l$  grid cell to a position partially within four adjacent cells.

advection of a block of material with a uniform concentration distribution. In analogy to the one-dimensional advection procedure, we define (suppressing the grid element subscripts  $l, m$ )

$$P_x = [1 + R_x - 2(F_x + \sigma_x)] / (2R_x),$$

$$P_y = [1 + R_y - 2(F_y + \sigma_y)] / (2R_y),$$

where the new subscripts  $x$  and  $y$  denote coordinate directions. Then, for the case illustrated in Fig. 6, where  $0 < P_x, P_y < 1$ , the contribution to the new concentrations at each of the four grid cells sharing the material after advection is

$$C_{m+1,l}^{T+1} = C_{m,l}^T P_x (1 - P_y), \quad (11a)$$

$$C_{m,l+1}^{T+1} = C_{m,l}^T (1 - P_x) P_y, \quad (11b)$$

$$C_{m+1,l+1}^{T+1} = C_{m,l}^T P_x P_y, \quad (11c)$$

$$C_{m,l}^{T+1} = C_{m,l}^T (1 - P_x) (1 - P_y). \quad (11d)$$

The rules for advection for  $P < 0$  or  $P > 1$  follow those derived for one-dimensional advection as do the expressions for calculating the first and second moments. Since the zeroth through second moments are generally evaluated from the concentration distributions advected from more than one adjacent cell, the computation procedure adopted logically determines which neighboring cells contribute to the moment calculations and computes  $\sum C_i$ ,  $\sum C_i F_i$ ,  $\sum C_i R_i^2$ , and then the new values for each element; thus, we have

$$C^{T+1} = \sum C_i \quad (12)$$

$$F^{T+1} = \frac{\sum C_i F_i}{C^{T+1}}, \quad (13)$$

$$(R^{T+1})^2 = \frac{\sum C_i R_i^2}{C^{T+1}} + 12(F^{T+1})^2. \quad (14)$$



Simple rectangular concentration distributions will be advected without distortion in a uniform velocity field by the above scheme. The variance of the distribution will, in all cases, be maintained. For curved velocity fields, accuracy can be retained by interpolation of the velocity vectors at the beginning and end positions of the advection steps.

### b. Treatment of horizontal diffusion

As discussed in Sections 2 and 3, horizontal diffusion will generally be of second-order importance to the dispersion of emissions from large area-type sources. However, in some applications it may be necessary to treat horizontal diffusion, especially situations where sub-grid-scale contributions from point sources or line-source segments are included. The conventional centered-difference scheme for simulation of diffusion, illustrated by Eq. (10), implicitly assumes uniform concentrations within each cell. The use of the zeroth, first and second moments of intracellular concentration distribution in the advection scheme allows retention of some sub-grid-scale details of the distribution. In particular, as illustrated in Fig. 6, the distributions may not be centered and may not completely fill the cell. In order to treat horizontal diffusion in a consistent manner, and to allow retention of sub-grid-scale detail, it is necessary to adopt an alternative procedure to simulate the diffusion process. A suggested treatment which involves increasing the variance of the concentration distribution as a function of the diffusion rate appears in the Appendix.

## 6. Summary

In modeling urban air pollution transport, it is important to treat emissions and dispersion consistently in light of the uncertainties associated with the description of turbulent processes, the determinations of other meteorological inputs, and with the estimation of emission rates. In addition, it is desirable that models be simple enough to allow analysis of the computation results in terms of the atmospheric physics involved. Thus, models should be free from artificially introduced errors such as those associated with systematically poor approximations to source geometries or those associated with the numerical computation scheme. The model presented here is simple in concept. It simulates the transport of pollutants in the fundamental manner of diffusing them in time and advecting them with the local wind velocity. Area-type source emissions are handled in a manner which utilizes conventional source inventories to good advantage. Special procedures utilizing moments of the concentrations distribution in the numerical calculation insure good resolution of concentration changes with time and space. Specific application of the model to urban air pollution phenomena will be reported in a separate paper.

**Acknowledgments.** We gratefully acknowledge the assistance of Mrs. Mary Ann Penney, who performed many of the necessary calculations, and R. Paul Larkin who has made the illustrations.

The research reported in this paper was supported by the Air Pollution Control Office of the Environmental Protection Agency under Research Grant AP 01013 and Training Grant AP 00003, and by the ASARCO Foundation, New York, N. Y.

## APPENDIX

### Numerical Simulation of Diffusion by Increasing Distribution Variances

Dispersion processes increase the variance  $V^2$  of any concentration distribution. For Fickian diffusion  $V^2 \propto Kt$ , and thus

$$\frac{dV^2}{dt} = 2K.$$

The scaled second moment will increase each time step according to

$$\Delta R^2 = 24K\Delta t / \Delta x^2. \quad (A1)$$

Since the scaled second moment is available from the computation scheme for advection, it is convenient to use the above property to simulate horizontal diffusion. To derive the procedure, we examine Fickian diffusion of material from a finite region of uniform concentration. The continuum distribution which results after a time increment  $t = \Delta t$ , as shown in Fig. 7a, is given by

$$C(s,t) = \frac{C_0}{2} \left\{ \operatorname{erf} \left[ \frac{(R/2) - s}{2(K\Delta t)^{1/2}} \right] + \operatorname{erf} \left[ \frac{(R/2) + s}{2(K\Delta t)^{1/2}} \right] \right\}, \quad (A2)$$

where  $s$  is the distance from the center of the distribution. This continuum process is simulated by a simple transfer of blocks of material (Fig. 7b) such that the amount of material transferred is the same and the resulting distribution variance increases by the same amount. Integrating (A2) to obtain the mass transferred to an adjacent cell in Fig. 7a, yields [for small  $(K\Delta t)/(R^2\Delta x^2)$ ]  $\Delta M = C_0(K\Delta t/\pi)^{1/2}$ . The mass transferred in the finite-element process is  $D\delta\Delta x$  and the variance of the distribution increases by an amount  $24D\delta^2\Delta x^2/C_0$ . Equating the mass transfer and the in-

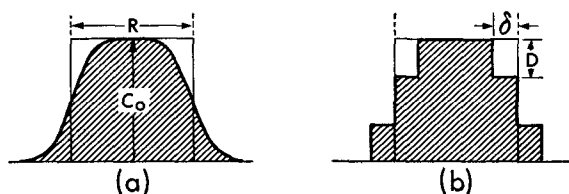


FIG. 7. Fickian diffusion from a region of initially uniform concentration of width  $R$  (a) and simulation by finite-element transfer (b).

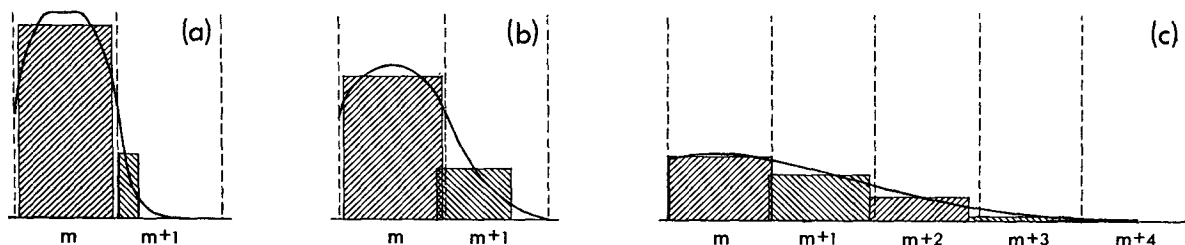


FIG. 8. Comparison of computed finite-element concentration distributions with analytic values as a function of increasing diffusion time,  $\tau = Kt/(\Delta x)^2$ , for  $\tau = 0.01$  (a),  $\tau = 0.09$  (b) and  $\tau = 0.81$  (c).

crease of variance, we find that

$$D/C_0 = 1/\pi, \quad \delta = (\pi K \Delta t / \Delta x^2)^{1/2}. \quad (\text{A3a, b})$$

The diffusive process can now be simulated by the following procedure:

1) Increase the product of the mass times the scaled variance of the material distributions in each grid variance by an amount

$$(CR^2)_m = C_m \left( R_m^2 + \frac{24K\Delta t}{\Delta x^2} \right). \quad (\text{A4})$$

2) If the distribution with increased variance overlaps a grid element boundary, transfer the material appropriately. For example, if  $P^* = F_m + R_m/2 + \delta - 0.5$  is greater than zero, as illustrated in Fig. 7b, we have at the next time step:

$$C_m^{T+1} = C_m^T - P^* D, \quad (\text{A5a})$$

$$(CF)_m^{T+1} = (CF)_m^T - P^* D(P^* + 1)/2, \quad (\text{A5b})$$

$$(CR^2)_m^{T+1} = (CR^2)_m^T - P^* D \left[ P^{*2} + 12 \left( \frac{1 + P^*}{2} \right)^2 \right], \quad (\text{A5c})$$

$$C_{m+1}^{T+1} = C_{m+1}^T + P^* D, \quad (\text{A5d})$$

$$(CF)_{m+1}^{T+1} = (CF)_{m+1}^T + P^* D(P^* - 1)/2, \quad (\text{A5e})$$

$$(CR^2)_{m+1}^{T+1} = (CR^2)_{m+1}^T + P^* D \left[ P^{*2} + 12 \left( \frac{P^* - 1}{2} \right)^2 \right]. \quad (\text{A5f})$$

Or, if  $P^* > \delta$ :

$$C_m^{T+1} = C_m^T - D\delta, \quad (\text{A6a})$$

$$(CF)_m^{T+1} = (CF)_m^T - D\delta(P^* + 1)/2, \quad (\text{A6b})$$

$$(CR^2)_m^{T+1} = (CR^2)_m^T - D\delta \left[ \delta^2 + 12 \left( \frac{1 + P^{*2}}{2} \right) \right], \quad (\text{A6c})$$

$$C_{m+1}^{T+1} = C_{m+1}^T + D\delta, \quad (\text{A6d})$$

$$(CF)_{m+1}^{T+1} = (CF)_{m+1}^T + D\delta(P^* - 1)/2, \quad (\text{A6e})$$

$$(CR^2)_{m+1}^{T+1} = (CR^2)_{m+1}^T + D\delta \left[ \delta^2 + 12 \left( \frac{P^* - 1}{2} \right)^2 \right]. \quad (\text{A6f})$$

Fig. 8 illustrates the results of continued application of this procedure to simulate Fickian diffusion of an initially rectangular concentration distribution in a zero-velocity field.

The simulation procedure described above is not limited to simple  $K$  theory. For example, dispersive processes where the variance increases as a function of the horizontal scale of the concentration distribution within a grid element can be specified by substitution of an appropriate expression for  $K$  in Eqs. (A1), (A3b) and (A4). In this way, empirically determined plume growth rates, such as those available in Turner (1969) or Smith (1968), may be used to model the dispersion of sub-grid-scale plumes.

## REFERENCES

- Calder, K. L., 1969a: A narrow plume simplification for multiple urban source models. Unpubl. ms., Environmental Protection Agency, Research Triangle Park, N. C., 11 pp.
- , 1969b: The numerical solution of atmospheric diffusion equations by finite-difference methods. Tech. Memo. 138, Department of the Army, Fort Detrick, Md.
- , 1970: Some miscellaneous aspects of current urban pollution models. *Proc. Symp. Multiple-Source Urban Diffusion Models*, Publ. AP-86, Environmental Protection Agency, Research Triangle Park, N. C.
- Crowley, W. P., 1968: Numerical advection experiments. *Mon. Wea. Rev.*, **96**, 1–11.
- Egan, B. A., and J. R. Mahoney, 1971: A numerical model of urban air pollution transport. *Reprints of Papers, Conf. Air Pollution Meteorology*, Raleigh, N. C., Amer. Meteor. Soc.
- Fortak, H. G., 1970: Numerical simulation of the temporal and spatial distributions of urban air pollution concentration. *Proc. Symp. Multiple-Source Urban Diffusion Models*, Publ. AP-86, Environmental Protection Agency, Research Triangle Park, N. C.
- Gifford, F. A., 1961: Use of routine meteorological observations for estimating atmospheric dispersion. *Nuclear Safety*, **2**, No. 4, 47–51.
- , and S. R. Hanna, 1971: Urban air pollution modelling. *Proceedings of the Second International Air Pollution Conference*, International Union of Air Pollution Prevention Associations, New York, Academic Press.

- Hilst, G., 1970: Sensitivities of air quality prediction to input errors and uncertainties. *Proc. Symp. Multiple-Source Urban Diffusion Models*, Publ. AP-86, Environmental Protection Agency, Research Triangle Park, N. C.
- Mahoney, J. R., 1970: Models for the prediction of air pollution. Report for the Organization for Economic Cooperation and Development, Paris.
- , and B. A. Egan, 1971: A mesoscale numerical model of atmospheric transport phenomena in urban areas. *Proceedings of the Second International Air Pollution Conference*, International Union of Air Pollution Prevention Associations, New York, Academic Press.
- Molenkamp, C. R., 1968: Accuracy of finite-difference methods applied to the advection equation. *J. Appl. Meteor.*, 7, 160-167.
- Moses, H., 1970: Mathematical urban air pollution models. Rept. ANL/ES-RPY-001, Argonne National Laboratory.
- Neiburger, M., and H. C. Chin, 1970: Numerical simulation of diffusion, transport and reactions of air pollution. *Project Clean Air Task Force Assessments*, Vol. 4, Section 2, University of California, Los Angeles.
- Panofsky, H. A., 1969: Air pollution meteorology. *Amer. Scientist*, 57, 269-285.
- Pasquill, F., 1961: The estimation of the dispersion of windborne material. *Meteorology Mag.*, 90, No. 1063, 33-49.
- , 1962: *Atmospheric Diffusion*. New York, Van Nostrand, 297 pp.
- , 1970: Prediction of diffusion over an urban area—Current practice and future prospects. *Proc. Symp. Multiple-Source Urban Diffusion Models*, Publ. AP-86, Environmental Protection Agency, Research Triangle Park, N. C.
- Randerson, D., 1971: A numerical experiment in simulating the transport of sulfur dioxide through the atmosphere. *Atmos. Environ.* (in press).
- Shieh, L. J., B. Davidson and J. P. Friend, 1970: A model of diffusion in urban atmospheres: SO<sub>2</sub> in greater New York. *Proc. Symp. Multiple-Source Urban Diffusion Models*, Publ. AP-86, Environmental Protection Agency, Research Triangle Park, N. C.
- Sklarew, R. C., 1970: Preliminary report of the S<sup>3</sup> urban air pollution model simulation of carbon monoxide in Los Angeles. Systems, Science and Software, Inc., LaJolla, Calif.
- Smith, M., 1968: *Recommended Guide for the Prediction of the Dispersion of Airborne Effluents*. New York, Amer. Soc. Mech. Engr.
- Stern, A. C., 1970: Editor, *Proc. Symp. Multiple-Source Urban Diffusion Models*. Publ. AP-86, Environmental Protection Agency, Research Triangle Park, N. C.
- Turner, D. B., 1969: Workbook of atmospheric dispersion estimates. Publ. 999-AP-26, Public Health Service, Washington, D.C.
- Wallington, C. E., 1968: Numerical solution of atmospheric diffusion equations. *Sci. Papers*, No. 28, Meteorological Office, London.